Determination of limiting current density and current efficiency

in Electrodialysis units

Mariagiorgia La Cerva[a], Luigi Gurreri[a*], Michele Tedesco[b], Andrea Cipollina[a], Michele Ciofalo[a], Alessandro Tamburini[a], Giorgio Micale[a]

[a] *Dipartimento dell'Innovazione Industriale e Digitale (DIID), Università degli Studi di Palermo (UNIPA) – viale delle Scienze Ed. 6, 90128 Palermo, Italy*
[b] *Wetsus, European Centre of Excellence for Sustainable Water Technology, Oostergoweg 9, 8911 MA Leeuwarden, The Netherlands*

Abstract

A crucial parameter for the design and operation of electrodialysis (ED) units is the limiting current density (LCD). In the literature, this is often identified with the diffusion-limited current density, which depends on concentration polarization and corresponds to the complete solute depletion in the solution layer adjacent to the membrane. Current-voltage curves obtained from measurements with electrodes in direct contact with the spacer are consistent with this interpretation and exhibit a linear region followed by a horizontal plateau identifying LCD. However, current-voltage curves of real ED systems show more complex trends, with a reduced-slope tract instead of a plateau and a third region in which the current increases more markedly (overlimiting current). The phenomena involved in the limiting region are not yet totally characterized and the determination of LCD in ED units is still ambiguous, although several methods have been proposed so far. In the present work, in order to explore the issues related to the identification of LCD, we performed *in situ* measurements on ED units, assessing the influence of operating conditions and validating a

simplified process simulator, which was then used for further investigation. A new method to determine LCD, based on the current efficiency, is proposed and compared with other methods presented in the literature. A second limiting quantity is also identified, i.e. the critical current density, at which there is no desalination, and a method for its assessment is proposed.

Key words:

electrodialysis, limiting current density, current efficiency, concentration polarization, ion exchange membrane

*Corresponding author; email: luigi.gurreri@unipa.it

1   Introduction

Electrodialysis (ED) is a membrane process known since 1890, but applied for water desalination only since the 1950s [1–3], when the first suitable ion-exchange membrane were commercially available [4,5]. An ED stack, illustrated in Figure 1a, consists of the repetition of a periodic unit, called cell pair (Figure 1b), which includes a cation exchange membrane (CEM), a diluate compartment, an anion exchange membrane (AEM) and a concentrate compartment. The spacing between membranes is maintained by inserting polymeric spacers. Those with overlapped or woven filaments are the most frequently used in membrane processes [6].
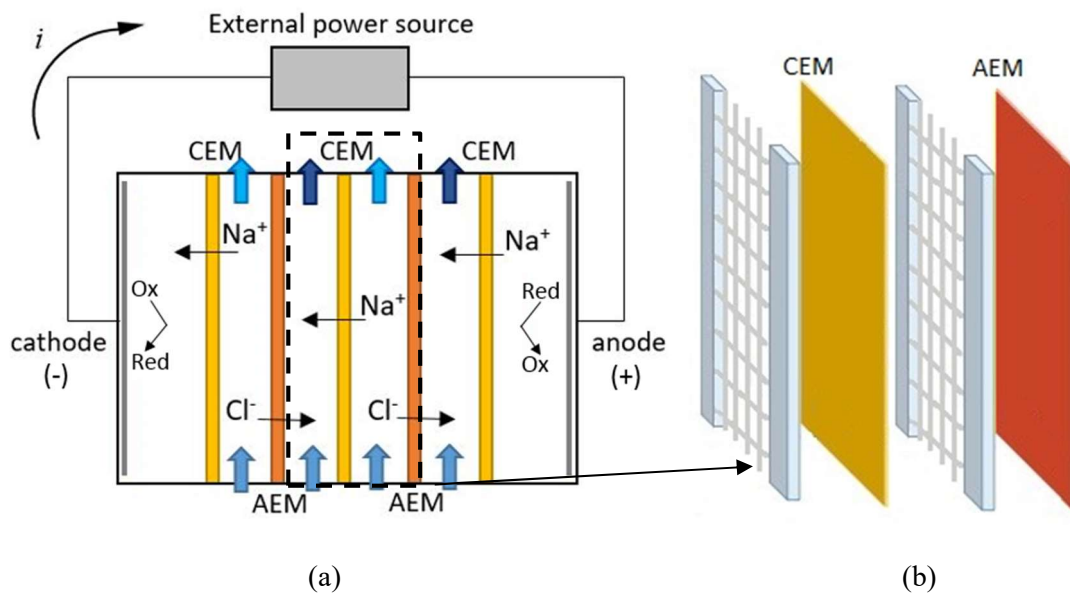

(a)   (b)

Figure 1. Schematic representation of a) ED stack and b) cell pair in a parallel flow configuration.

Electrodialysis has become of increasing relevance in the last decade, e.g. in the production of high-quality industrial process water and the treatment of industrial effluents [7,8]. A combination of ED and brackish water reverse osmosis (BWRO) was proposed by Galama

et al. [9] as an alternative to seawater reverse osmosis (SWRO). The application of multistage ED to seawater desalination is also currently studied [10].

The performance of the ED process is improving due to the research efforts towards producing high-performing ion-exchange membranes [11]. However, real membrane properties still have an important role in limiting the performances, especially non-ideal permselectivity and water permeability. The minimum energy consumption, expected for seawater desalination, increases by a factor of 3 if co-ions flux is considered and by about 10% when also the water flux is considered [12,13]. Aside from the membrane properties, the performance of an ED stack can be affected by other parameters or phenomena, among which the most relevant is concentration polarization.

According to the IUPAC Recommendations, concentration polarization is defined as "a concentration profile that has a higher (lower) level of solute nearest to the upstream membrane surface compared with the more-or-less well-mixed bulk fluid far from the membrane surface" [14]. An example of concentration profiles in the concentrate and diluate compartments is reported in Figure 2a.

These profiles arise because the kinetics of transport in solutions and in membranes are different, which leads to enrichment and depletion layers next to the membranes. This phenomenon can also be explained by considering the transport numbers, which are higher in membranes than in solutions ($T > t$): moving from the solution to the membrane, the migrative flux of counter-ions increases and a concentration gradient arises in the liquid phase [15].
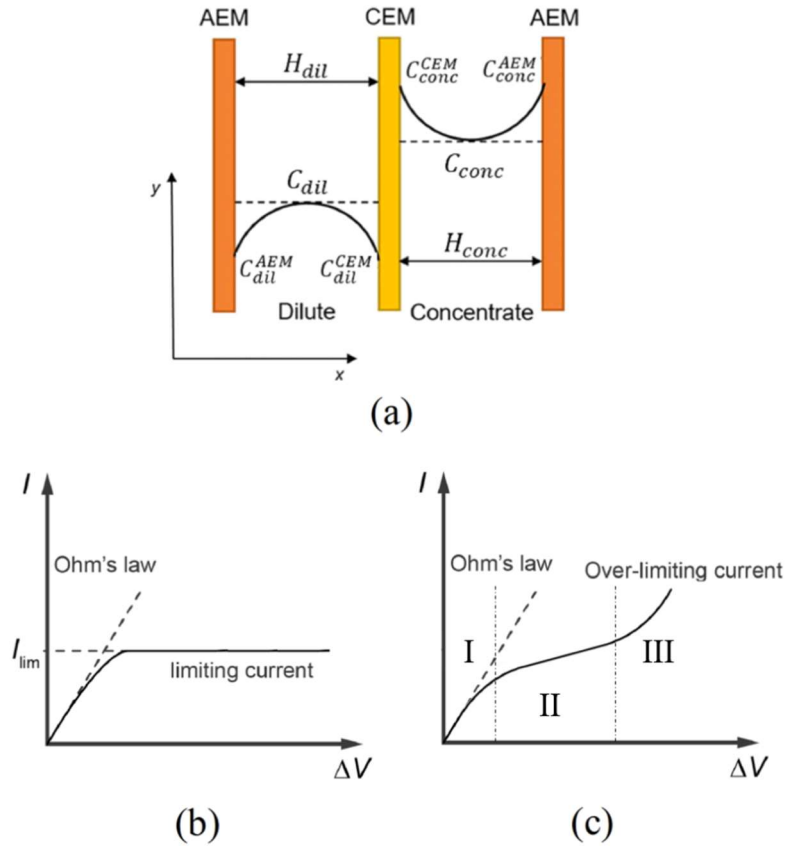
Figure 2. (a) Concentration profiles in a cell pair; (b) current-voltage curve according to the classical theory of concentration polarization [16]; (c) typical current-voltage curve observed in working ED unit [17].

Observing the diluate channel, the concentration at the membrane surface decreases and, according to the classical theory of concentration polarization in an electroneutral solution [18], when the electrolyte concentration approaches zero, the diffusion-limited current density is reached [19,20]. This condition corresponds to a plateau in the current-voltage curve (Figure 2b).

According to this theory, the first predictions of the limiting current density was proposed by Peers [21] in 1956. In the Peers equation (see Table 1) δ is the diffusion boundary layer thickness. This is often defined as the distance from the membrane to the cross point of the tangents drown to the concentration profile at the interface and in the bulk solution [22]. In

the literature, the Lévêque equation [23,24] is more commonly adopted: it is derived from the Peers equation and the Graetz-Lévêque theory of developing laminar flow through spacerless channels, and it is valid for membranes characterized by a short length, i.e., when $(LD)/(H^2 u) < 10^{-2}$, and homogenous surface [25]. Among the most recent models proposed in the literature to estimate LCD, Geraldes and Afonso [26] considered the electrodialysis of multi-ionic solutions: using a linearized form of the Nernst–Planck equation together with the electroneutrality condition at the solution/membrane interface, they deduced an explicit expression of LCD, which requires the effective diffusivity of the multi-ionic solution. Nakayama *et al.* [27] started from the Nernst-Planck equation, which they reduced to a convection-diffusion transport equation with an effective diffusion coefficient by eliminating the electrophoresis term. This equation was then applied in the boundary layer, by using the principle of similarity of the classical boundary layer theory [28], in order to obtain asymptotic solutions for concentrations, limiting current density and stack voltage, for long and short ED channels.

All the above models can predict the plateau in the current-voltage curve (Figure 2b), which can be observed only in simple electrochemical cells in which a single solution-filled channel is limited by two electrodes. In these cases, the diffusion-limited current density is univocally determined by the plateau. When ion exchange membranes (IEMs) are present, as in the case of real ED stacks, there is no true saturation of current: as illustrated in Figure 2c, the current does not exhibit a marked plateau but rather a region of slow increase which merges without a sharp transition with a third region, the overlimiting region [29]. The appearance of this last region was initially attributed to the loss of permselectivity and the transport of H^+ and OH^-, produced by a water splitting reaction. These phenomena, however, were later identified as non-significant contributions to the overlimiting current: in fact, even for currents much larger than the diffusion-limited value, charge is mainly transported by salt

ions and the contribution of water splitting is minor [30]. The main reason of the overlimiting current was rather found in membrane surface non-uniformity and in electroconvection phenomena [22,31,32]. The second region, still called plateau region, appears at much lower current values than the diffusion-limited [31]. For example, Krol *et al.* [33,34] measured the limiting current density and the transition time in a Plexiglas™ membrane cell with six separate compartments; the experimental results were lower than that calculated using theoretical expressions such as the Peers equation. The micro-scale mechanisms responsible for this behaviour are not yet fully understood; it is widely believed that some of the phenomena that cause overlimiting currents (e.g. membrane non-uniformity, electroconvection, *etc.*) may be implied also at this earlier stage. Rubinstein *et al.* [30] observed that when electroneutrality is imposed, as assumed in classical theory of concentration polarization [18], the current-voltage curve can not exhibit the S-shape with an overlimiting region, typical of ED systems. More realistic current-voltage curves can be predicted if the electroneutrality condition is replaced by the full Poisson equation for the electrical potential [35]. Moreover, from the experiments carried out by Shaposhnik *et al.*[36], it can be observed that, when the limiting current is reached, the concentration at the membrane-solution interface is not zero but rather attains a finite minimum value.

As a consequence of this departure from the purely diffusion-controlled behaviour, the identification of a limiting current density in real ED stacks is not obvious. However, the concept of LCD is still useful for a number of reasons. First, since water splitting can lead to scaling or fouling, it is important to operate with a safe margin below the corresponding conditions. Second, since the attainment of LCD can be associated with a maximum in current efficiency (as will be discussed below), a knowledge of this quantity facilitates the efficient design of ED equipment [37]. Therefore, a predictive model for LCD should be

implemented into any simulation model for the design an performance prediction of ED systems [38].

Table 1. Summary of theoretical and empirical correlations presented in the literature.

Author (year)	Equation	Ref.
Peers (1956)	$$i_{lim} = \frac{FDC}{\delta(T-t)}$$	[21]
Lévêque (1973)	$$i_{lim} = 1.47\frac{FDC}{H(T-t)}\left(\frac{H^2 u}{LD}\right)^{1/3}$$	[23,24]
Geraldes and Afonso (2010)	$$i_{lim} = F\frac{k_{c,eff}}{D_{eff}}z_1 D_1\left(C_{1,b} + C_{2,b} + C_{3,b}\right)$$	[26]
Nakayama et al (2017)	$$i_{lim} = 1.772 F\bar{C}_d(0)\left(\frac{\bar{u}_d}{L}\varepsilon D_e\left(1 + \xi\frac{\bar{u}_d W}{D_e}\right)\right)^{1/2} \ for \ \frac{\bar{u}_d W^2}{\varepsilon D_e\left(1 + \xi\frac{\bar{u}_d W}{D_e}\right)L} \gg 1$$	[27]
Lee et al (2002, 2006)	$$i_{lim} = aCu^b$$	[39,40]
Tanaka (2004, 2005)	$$i_{lim} = (m_1 + m_2 u_{out})C_{out}^{'n_1 + n_2 u_{out}}$$	[41,42]

As an alternative to physically-based models, purely empirical correlations for the LCD can be found in the literature, often in the form of power laws. Table 2 summarizes theoretical and empirical correlations presented in the literature. Lee *et al.* [39] obtained an equation for the limiting current in which the coefficients are quite constant in a relative wide concentration range of the feed solution except for very low concentrations, but they are affected by the hydrodynamic conditions, including the flow velocity [40]. Instead of using the inlet or average velocity, Tanaka [42] found a correlation in which the coefficient and the exponent are functions of the outlet velocity of the dilute solution. However, correlations are usually calibrated against experiments carried out in specific electrochemical cells, often

using only one ion exchange membrane and one solution [29,31,33,34,41,43–45]. In other cases, the LCD is measured in simplified or real ED systems [26,37,39,40,42,46].

Since the "practical limiting current density" in ED is not identifiable by a marked plateau, several alternative methods, many of which of a graphical nature, have been proposed in the literature so far. Isaacson and Sonin [37] proposed to consider as a measure of the limiting current, the intersection between a straight line extrapolated from the linear (Ohmic) region and the tangent drawn past the turning point in the region in which the current tends to level off. In 1959, Cowan and Brown [47] were the first who plotted the apparent resistance $\Delta V/i$ against the reciprocal current density $1/i$ to identify the limiting current density. They designated as LCD the point at which the trend line with a negative slope cuts that with a positive slope. Although several methods have been proposed and many efforts have been made so far, the determination of the LCD is still ambiguous.

The aim of this paper is to compare the state-of-the-art experimental techniques and graphical methods to determine the LCD in working ED systems. In order to study these aspects, measurements on ED units were carried out under a variety of experimental conditions and the LCD values obtained by different data processing methods were compared.

2   Experimental setup and methods

2.1 Experimental set-up

A cross flow ED stack (REDstack, The Netherlands), consisting of 10 cell pairs, with an active area of 10×10 cm^2, was tested. The membranes investigated were supplied by Fujifilm Manufacturing Europe BV (The Netherlands) and their properties are reported in Table 2. Between the membranes, woven spacers, 155 μm thick and provided with gasket, are placed. These spacers have a pitch to height ratio $l/H = 2$ and a porosity of 75%. The electrode rinse

solution (0.3 M $K_3Fe(CN)_6$; 0.3 M $K_4Fe(CN)_6 \cdot 3H_2O$; 0.25 M NaCl) is pumped into the stack by a peristaltic pump (Masterflex Cole-Palmer) with a flow rate of 180 ml/min. A similar pump is used for the feed solutions, for which a one-pass flow arrangement was used. Pressure transducers (Endress+Hauser Cerabar M) were installed at the inlet of each stream, and conductivity was measured at the inlet and the outlet by a portable conductivity-meter (WTW 340i).

Table 3. Ion exchange membranes properties (data provided by manufacturer).

	Permselectivity[a] [%]	Water permeability [ml/m²hbar]	IEC [meq/g]	Resistance[b] [Ω cm²]	Thickness (dry) [μm]	Thickness (wet) [μm]
AEM FujiFilm	97	8.0	2.85	1.77	120	130
CEM FujiFilm	98	8.0	2.9	1.89	120	130

[a] Membrane potential measured over the membrane between 0.05 M and 0.5 M KCl solutions at 25°C.

[b] Measured in 2 M NaCl solution at 25°C.

We performed experiments with solutions prepared using demineralised water and technical grade NaCl with concentrations from 0.5 to 60 g/l, encompassing the whole range of outlet concentrations expected in a real ED plant. We used different inlet concentrations in the two compartments in order to simulate the end part of a long stack or the last stage of a multistage configuration. For each couple of inlet concentrations, solutions velocities in the range 0.25 – 2 cm/s were imposed and were kept equal in the concentrate and diluate compartments.

2.2 Experimental methods

The prescriptions recommended in reference [48] for electrodialysis experiments were followed. For all measurements, a potentiostat/galvanostat was used (Ivium Technologies, The Netherlands). The current was increased stepwise, where each current step duration was at least four times the residence time of feed water in the system (typically 300 s) to ensure steady-state conditions, and it was preceded and followed by a stage of open circuit (open circuit voltage, OCV) [49].

Figure 3a shows an example of a stepwise function of the current during a typical test, and the corresponding voltage response. The current-voltage curve (Figure 3b) is obtained by taking, for each current step, the stationary voltage value or the mean value in the presence of oscillations.
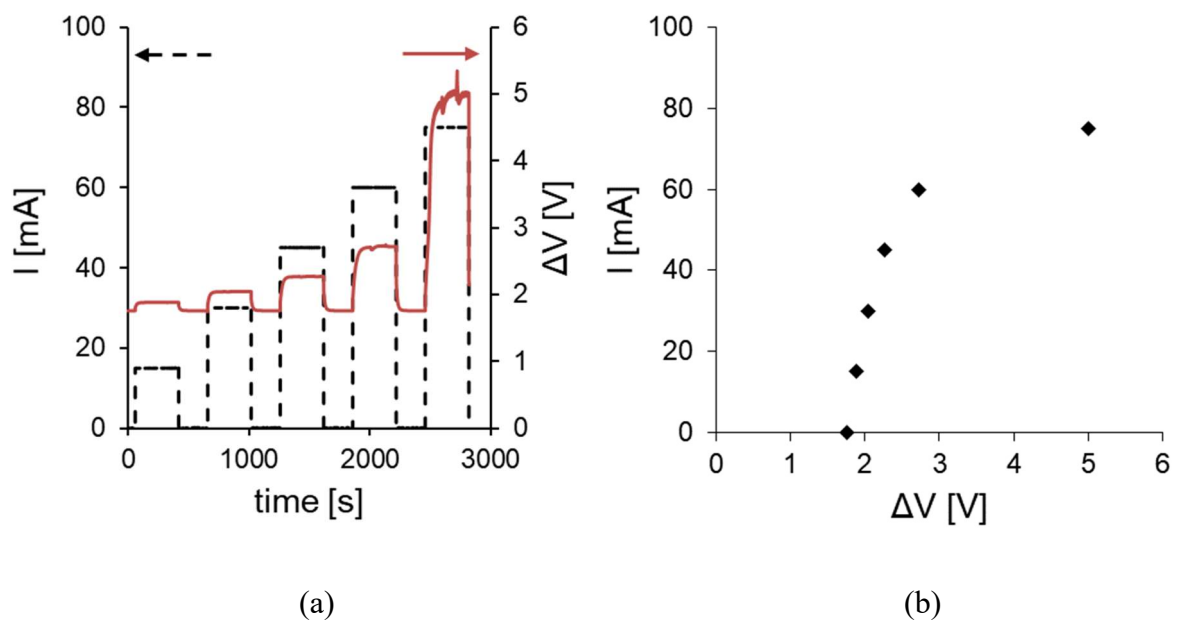

(a)   (b)

Figure 3. a) Applied current (dashed line) and corresponding voltage (continuous line) vs time; b) current-voltage curve.

3 Modelling

As demonstrated in a previous work [50], in modelling complex processes, such as ED or reverse electrodialysis (RED), a good compromise between accuracy and computational load is to use a simplified (e.g., one-dimensional) model of the stack, which incorporates local results (e.g. friction coefficients and mass transfer coefficients or polarization factors) computed by fully three-dimensional models.

In our one-dimensional model, we simulate the change in bulk concentrations along the flow direction by appropriate salt and water balance equations along the axial coordinate (y) (Figure 2a). The governing equations of the model are essentially the same as those reported for reverse electrodialysis in [50] with an appropriate change of some signs. The only difference is in the assessment of the migrative flux which, for monovalent ions as in the case of NaCl, can be expressed as:

$$N_{S,MIG} = \frac{i}{F}[t^{CEM} - (1 - t^{AEM})] \qquad (1)$$

in which the term in square brackets is a correction for co-ion back diffusion across the membranes in ED. Here, t^{AEM} and t^{CEM} are the transport numbers in membranes, calculated as $t^{IEM} = 0.5(\alpha^{IEM} + 1)$ where α is permselectivity and *IEM* stays for *AEM* or *CEM*.

Other non-ideal phenomena considered in the model are salt diffusion, electro-osmotic and osmotic fluxes. In the evaluation of osmotic pressures, Pitzer's correlations are adopted [51,52].

The concentration variation in the direction orthogonal to the membranes (x) is modelled by polarization coefficients θ_{conc}^{IEM}, θ_{dil}^{IEM}. These are functions of bulk concentrations and salt flux, and are defined as:

$$\theta_{conc}^{IEM} = C_{conc}/C_{conc}^{IEM}; \qquad \theta_{dil}^{IEM} = C_{dil}^{IEM}/C_{dil} \qquad (2)$$

Polarization coefficients are computed from the Sherwood numbers:

$$\theta_{conc}^{IEM} = \frac{C_{conc}}{C_{conc} + \dfrac{N_S^{IEM}}{Sh_{conc}} \dfrac{2H_{conc}}{D_{conc}}} ; \qquad \theta_{dil}^{IEM} = 1 - \frac{N_S^{IEM}}{C_{dil}Sh_{dil}} \frac{2H_{dil}}{D_{dil}} \qquad (3)$$

Each Sherwood number is defined as

$$Sh_{SOL} = \frac{N_S^{IEM}}{|C_{SOL} - C_{SOL}^{IEM}|} \cdot \frac{2H_{SOL}}{D_{SOL}} \qquad (4)$$

and depends on the Reynolds and Schmidt numbers and on the spacer's geometry, so that it can be predicted by CFD simulations independent of specific concentration values [53–55]. Alternative definitions of Sh have also been adopted in the literature, see e.g. ref. [56].

For the woven spacers adopted in the experiments, we obtained the following correlation:

$$Sh = -1.1918 \cdot 10^{-2} Re^2 + 2.90289 \cdot Re + 13.4528 \qquad (5)$$

where Re is the Reynolds number computed from the void, or approach, velocity and the hydraulic diameter of an empty plane channel, i.e. twice the channel thickness.

Eq. (5) was obtained for a 0.017M NaCl solution at 25°C, for which the Schmidt number is 586 [57,58]. These conditions were arbitrarily chosen as reference ones. In previous studies, different concentrations were simulated and it was shown that, in cases other than the reference one, the Sherwood number can be well approximated multiplying the Sherwood number computed for the reference concentration by $(Sc/Sc_{ref})^{1/2}$, where Sc and Sc_{ref} are the

Schimdt number at the given concentration and that at 0.017M, respectively [50]. Similarly, the temperature dependence of Sc might be taken into account.

Even if the experiments were carried out with a cross-flow stack, we assumed in the model a co-current flow which requires a simpler one-dimensional approach. It was shown [59] that the error thus made is small, especially if pressure drop in the channels and pumping power are not taken into account.

In regards to the Ohmic resistances, the areal resistance of a cell pair is calculated as the series of four resistances, i.e., two associated with the compartments and two with the membranes. The areal resistance of a spacer-filled channel, i.e. the solution compartment, can be well approximated as:

$$r_{SOL} = \frac{H_{SOL}}{\varepsilon \sigma_{SOL}} \tag{6}$$

where ε is the porosity of the given spacer and σ_{SOL} is the conductivity of solution, which is assumed to be a function of the bulk concentration [60]. For the Ohmic resistance of the membranes, we used an empirical correlation similar to that proposed in [50] with appropriate coefficients. Other parameters used in the model are: water permeability 8 ml/(m^2 h bar), salt diffusivity $3.7 \cdot 10^{-12}$ m^2/s, electrode (blank) resistance $2 \cdot 10^{-3}$ Ωm^2. Permselectivities and membrane resistances are computed as functions of concentration at 25°C, see Appendix in [50].

For given applied voltage ΔV, concentrations, dimensions of the stack, velocities in the channel, blank resistance (Ohmic resistance of the electrodic compartments) and membrane properties, the governing equations are solved by a finite difference method. To this purpose, the stack length is divided into N divisions (typically 50). The resulting set of algebraic equations was implemented into a MS Excel™ spreadsheet.

4 Results and Discussion

4.1 Comparison of methods for determining the LCD

As discussed in previous sections, different methods have been proposed in the literature to determine the experimental LCD in Electrodialysis. Figures 4a and 4c show the determination of LCD with 0.5 g/l for both solutions, while Figures 4b and 4d refer to 60 g/l and 0.5 g/l in the concentrate and diluate, respectively. First, we applied the method proposed by Isaacson and Sonin [37] (Figures 4a and 4b). As it can be seen from Figures 4a-b, the slope of the right side tangent is not uniquely determined and depends on the density of the available experimental data. LCD values of ~12.3 and 17.8 A/m^2 were obtained for the two test cases (a) and (b), respectively.

We also used the method proposed by Cowan and Brown [47] which identifies the LCD in the plot of the apparent resistance $\Delta V/i$ against the reciprocal current $1/i$ (Figures 4c and 4d). We obtained some plots (Figure 4c) in which the trend line for higher $1/i$ values (low current values) was almost horizontal. The values of LCD thus obtained were ~12.8 and 16.7 A/m^2, respectively, for test cases (c) and (d); these values are, especially in case (d), considerably different from those obtained by the Isaacson-Sonin method.
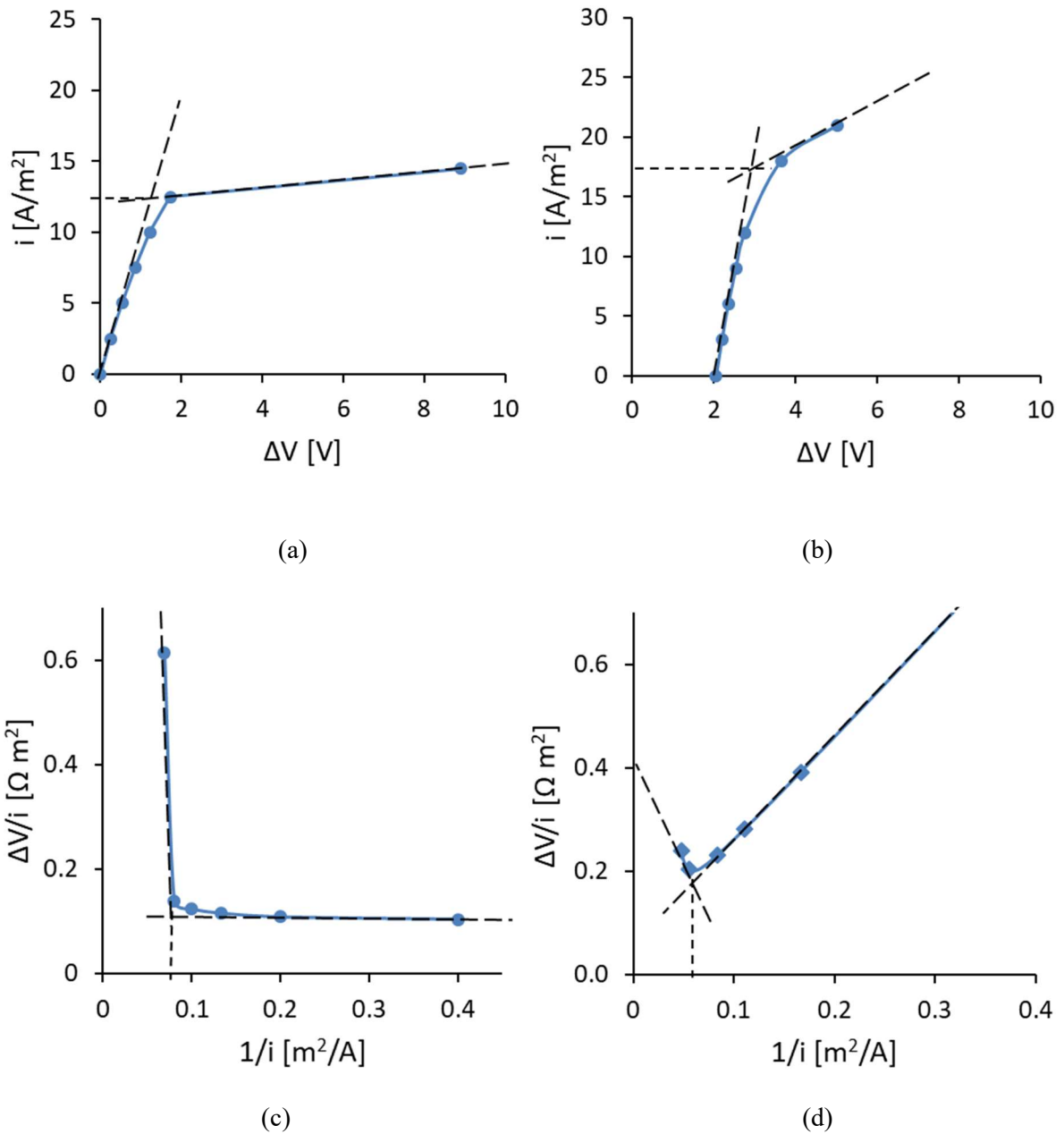
Figure 4. Graphs (a, b) Isaacson and Sonin method: current density vs applied voltage. Graphs (c, d) Cowan-Brown method: $\Delta V/i$ vs $1/i$. Symbols represent experimental data. These curves were obtained with NaCl solutions of: a) and c) equal concentration in both compartments, $C_{dil} = C_{conc} = 0.5$ g/l; b) and d) concentrate concentration $C_{conc} = 60$ g/l and diluate concentration $C_{dil} = 0.5$ g/l. Velocities were 1.5 cm/s in both compartments.

Mandersloot and Hicks [1], using the Cowan-Brown method, also observed quasi-horizontal regions in the $\Delta V/i$ vs. $1/i$ curve. In their experiments, they kept the concentration in the concentrate fixed while letting the diluate concentration vary, and concluded that this horizontal section appears because the membrane potential becomes negligible at high diluate concentrations. Our own experiments suggest that the $\Delta V/i$ versus $1/i$ curve flattens for $1/i \rightarrow \infty$ ($i \rightarrow 0$), as in Figure 4c, not when the diluate concentration is high, but rather when the difference ($C_{conc} - C_{dil}$) tends to zero, so that also the back electromotive force $V(i=0)$ (residual potential at zero current) tends to zero. This is illustrated by the current density-voltage curve of Figure 4a, which corresponds to Figure 4c. On the contrary, when ($C_{conc} - C_{dil}$) $\neq 0$, one also has $V(i=0) \neq 0$, as shown in the current density-voltage curve of Figure 4b. In this case, in the linear region (low electrical current) the applied voltage can be approximated (neglecting the influence of concentration polarization) as $V = V(i=0) + constant \times i$, and the ratio $\Delta V/i$ decreases as the current density i increases.

The methods illustrated in Figure 4 are the most used in the literature; however, as discussed above, they may lead to an ambiguous determination of the limiting current in some cases, because the choice of the "appropriate" tangent lines is difficult. Meng *et al.* [61] pointed out the uncertainties of these methods and proposed a new method, but only to determine the optimal operating current, which should be lower than the limiting current. They used the desalting efficiency η defined as the ratio $\frac{c_{dil}^{IN} - c_{dil}^{OUT}}{c_{dil}^{IN}}$. As the current increases, this parameter shows a maximum, which can be identified with the optimal operating current [61].

As an alternative to the desalting efficiency η, the current efficiency, or current utilization, λ [62] can be used to identify an optimal operating current. λ can be defined as:

$$\lambda = \frac{F\left(Q_{dil}^{IN} C_{dil}^{IN} - Q_{dil}^{OUT} C_{dil}^{OUT}\right)}{I} \qquad (7)$$

From the experimental values of current, flow rates and concentrations, we calculated λ and plotted it against the current density as illustrated in Figure 5. For all experimental tests, we observed that a maximum of λ always occurs in such plots. Up to a certain value of the current density i, the current efficiency increases so that the $C_{dil}^{OUT}(i)$ curve exhibits a negative curvature (downward concavity). When the current efficiency attains a maximum, the $C_{dil}^{OUT}(i)$ curve exhibits an inflection point (i.e., its curvature changes sign).
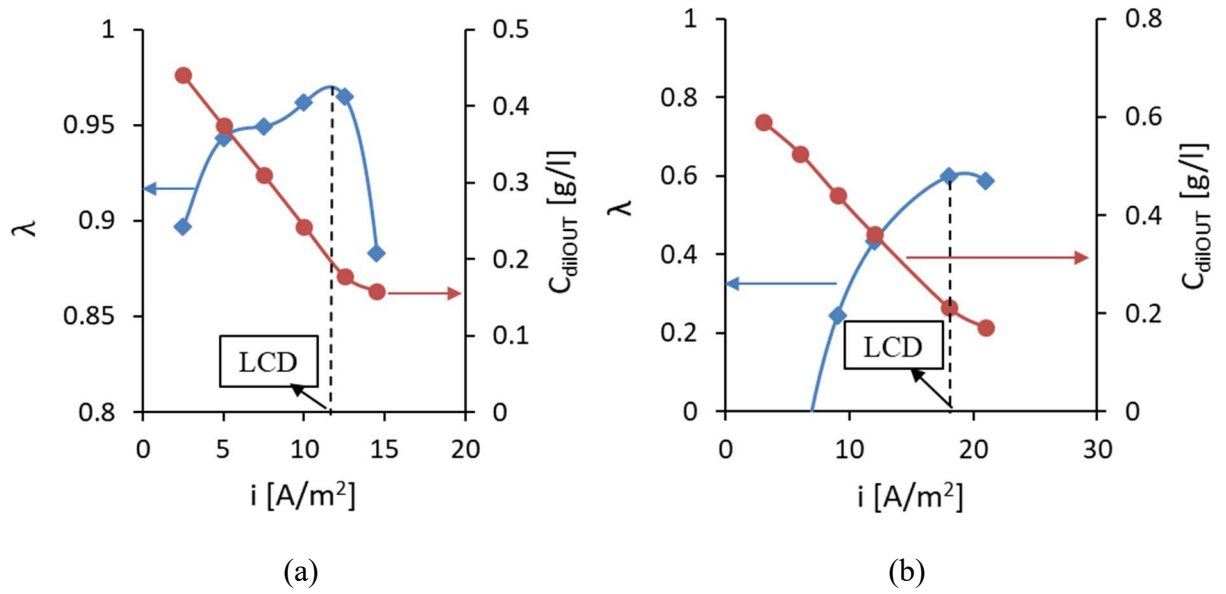

(a)   (b)

Figure 5. Current efficiency (diamonds) and outlet dilute concentration (circles) as function of current density. Symbols are experimental data (trend lines were drawn to guide the eye). Data were obtained with NaCl solutions of: a) equal concentration in both compartments, $C_{dil} = C_{conc} = 0.5$ g/l; b) concentrate concentration $C_{conc} = 60$ g/l and diluate concentration $C_{dil} = 0.5$ g/l. Velocities were 1.5 cm/s in both compartments.

Kwak *et al.* [63] also observed this trend of the current efficiency and stated that the maximum λ corresponds to the initial stage of the overlimiting region. More appropriately,

based on our results, we can identify the current density corresponding to the maximum λ with the LCD, obtaining values of 11.6 and 19.2 A/m^2 for the cases (a) and (b), respectively. Indeed, these values are very close to the above reported LCD values predicted by the Isaacson-Sonin or the Cowan-Brown (Figure 4) methods. As an advantage, the method based on the λ maximum is less ambiguous and has a more practical usefulness.

4.2 Effect of operating conditions

The theoretical and empirical correlations presented in the literature (Table 1) show a dependence of the LCD on the diluate concentration. This fact reflects the operating conditions used in the experiments in which often there is one solution in an electrochemical test section [29,31,33,34,41,43–45] or, even if an ED stack is used, the same solution is always fed into both the concentrate and the diluate compartments [26,37,39,40,42,46]. When the experiments are performed with the same inlet concentrations, one may conclude that LCD is only a function of the diluate concentration. However, in ED systems, different concentrations in the compartments can be found, especially near the outlet of the stack.

Figure 6 summarizes the experimental results by reporting LCD, as determined by using the maximum current efficiency method illustrated above, as a function of the solution velocity for different values of the concentration in the concentrate compartment. Figure 6a is for a diluate concentration of 0.5 g/l, while Figure 6b for a diluate concentration of 1 g/l. Data can be interpolated by power laws, as commonly found in the literature (see Table 1).

First, each graph confirms that, as commonly reported in the literature, LCD increases strongly with the solution velocity. Second, the comparison of the results in Figure 6a and Figure 6b, obtained with the same concentrate (30 g/l) and two different diluate concentrations (0.5 and 1 g/l, respectively), confirms that LCD increases with the diluate

concentration. Furthermore, the comparison of the different curves in each graph, obtained for the same diluate concentration but different concentrations in the concentrate, shows that LCD increases significantly also with C_{conc}. This effect, usually not considered in the literature, is probably caused by the fact that salinity in the concentrate compartment affects the diluate concentration due to non-ideal phenomena such as diffusion and osmosis.
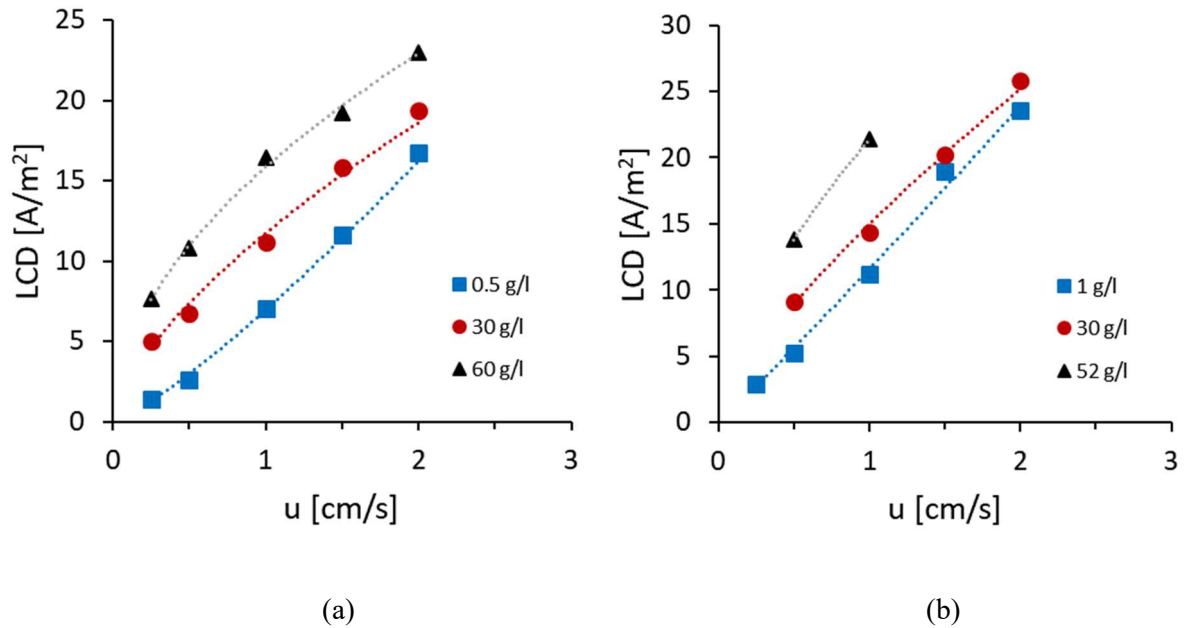

(a)   (b)

Figure 6. Experimental results obtained with 155 μm spacers: LCD as a function of the solution velocity for different values of the concentration in the concentrate compartment. a) concentration in the diluate C_{dil} = 0.5 g/l; b) concentration in the diluate C_{dil} = 1 g/l. Trendlines (power laws) are added to guide the eye.

4.3 Comparison of model predictions and experimental results

This section describes the comparison between our model predictions and experimental data. For example, Figure 7 reports experimental results for concentrate and diluate outlet concentrations and stack voltage as functions of the current density, and a comparison with the one-dimensional stack model described in Section 3.
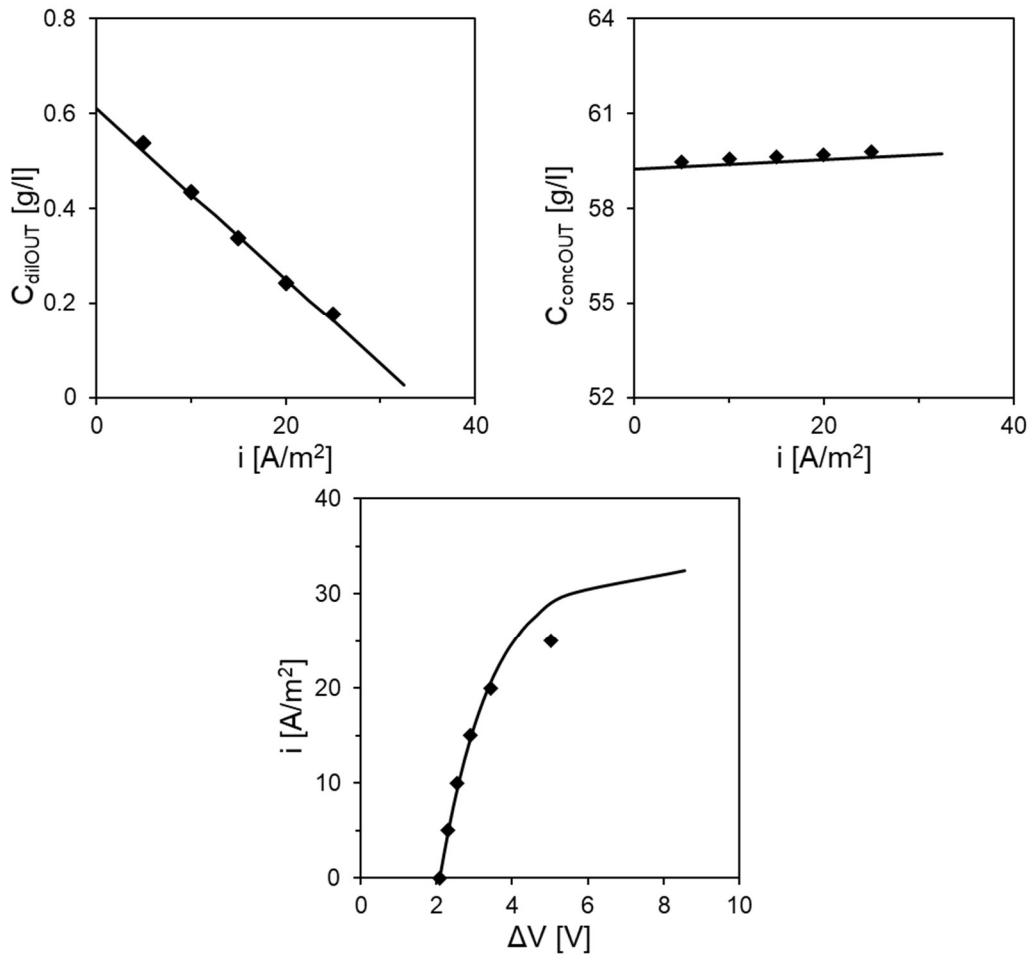
Figure 7. Diluate and concentrate outlet concentrations and stack voltage reported as functions of the current density. Experimental data (symbols) and simulation results (lines) are compared. Data were obtained using NaCl solutions with inlet concentrations of $C_{conc} = 60$ g/l in the concentrate and $C_{dil} = 0.5$ g/l in the diluate. The velocity was equal to 2 cm/s.

Overall, the model predictions are in good agreement with the experimental results; however, the limiting region of the current-voltage curve is not satisfactorily predicted. Several reasons can be invoked for this discrepancy. First, among the several non-ideal phenomena involved in ED, the model takes into account only salt diffusion and osmotic / electro-osmotic fluxes. Moreover, concentration polarization is computed from Sherwood numbers provided, in their turn, by CFD simulations in which the membrane surface is assumed homogenous and electroneutrality is imposed. These two assumptions lead to a plateau in the current-voltage

curve, determining the diffusion-limited current density, and do not consider the possible establishment of electroconvective motions [30,31]. Gurreri *et al.* [55] reported a good match between the Sherwood numbers obtained from their CFD simulations under the same assumptions and the Sherwood numbers experimentally deduced by Li *et al.* [6,64] and Koutsou *et al.* [65]. However, these experimental results were obtained with the spacer directly in contact with the electrode and, as explained above, this condition provides the theoretical diffusion-limited current density, which is higher than LCD in Electrodialysis.

4.4 Critical current density

Figure 8 reports diluate outlet concentrations as functions of the current density, by comparing experimental data (symbols) and simulation results (lines). The inlet concentrate / diluate concentrations are a) 30 g/l and 0.5 g/l; b) 60 g/l and 0.5 g/l. Five solution velocities, from 0.25 to 2 cm/s, are considered.

Observing the outlet concentration of the diluate channel for given inlet concentrations (Figure 8), a lower threshold of the current density, which we define as "critical current density" (CCD), can be observed: below this limit, the outlet concentration is higher than that of the input, while, above this limit, desalination is obtained. For example, in Figure 8a the inlet concentrations are 30 g/l in the concentrate and 0.5 g/l in the diluate but, for current densities below $\sim$3 A/m^2, the outlet diluate concentration is higher than 0.5 g/l. This is due to the osmotic and salt diffusion phenomena, which depend on the concentration difference between the two compartments.

2
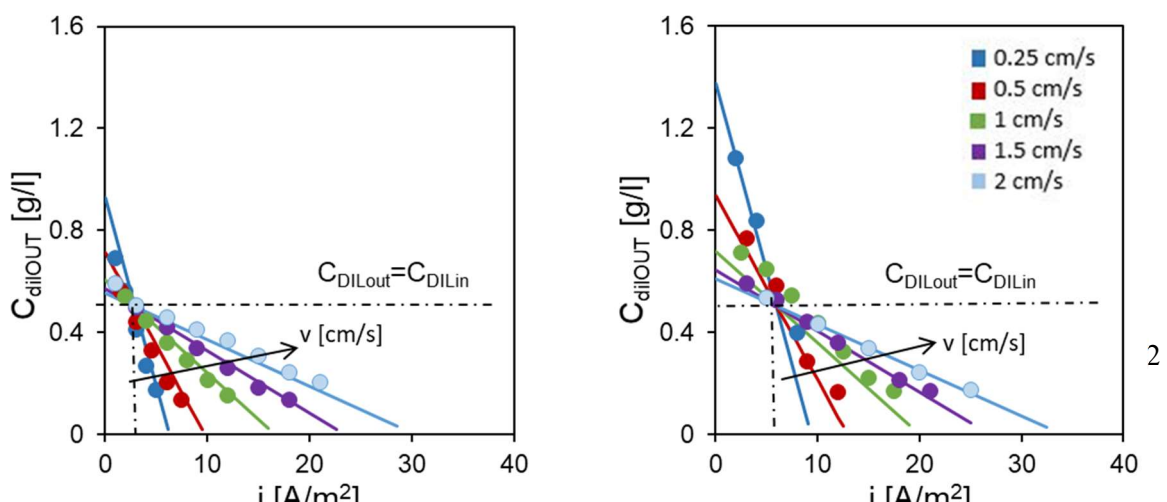
(a)   (b)

Figure 8. Diluate outlet concentration vs current density. Experimental data (symbols) and simulation results (lines) are compared. Five solution velocities are examined. NaCl solutions are characterized by concentrate / diluate inlet concentrations of: a) C_{conc} = 30 g/l and C_{dil} = 0.5 g/l; b) C_{conc} = 60 g/l and C_{dil} = 0.5 g/l.

When the concentration in the concentrate doubles, also the CCD doubles. For example, when the concentrate concentration is 60 g/l (Figure 8b), the CCD increases and becomes ~6 A/m². The curves at different velocities intersect all in a single point, i.e. the CCD does not depend on fluid velocities. This independence arises from the fact that the above-mentioned non-ideal phenomena (osmosis, diffusion *etc.*), which lead to a CCD, are not dependent on the solutions velocity. An equivalent way of expressing this concept is that transport phenomena in the direction of the flow (advection) and in the direction orthogonal to it and through the membranes (electromigration, diffusion, osmotic fluxes) can be decoupled, as stated by Sonin and Probstein [3].

Under critical current density conditions, the total salt flux going out from the dilute channel is zero, and the migrative flux, $N_{S,MIG}$, is equal and opposite to the diffusive flux, $N_{S,DIFF}$. The diffusive flux through a membrane pair can be expressed as:

$$N_{S,DIFF} = 2N_{S,DIFF}^{IEM} = 2\frac{D_m(C_{conc} - C_{dil})}{s_m} \qquad (8)$$

where D_m is the membrane salt diffusivity and s_m is the membrane thickness. Once the permselectivity and the membrane salt diffusivity are known, by combining Eq (1) and Eq (8) the CCD can be determined as:

$$CCD = \frac{2FD_m(C_{conc} - C_{dil})}{s_m[t^{CEM} - (1 - t^{AEM})]} \qquad (9)$$

For the membranes used in our experiments, the manufacturer provides a salt diffusivity of $4 \cdot 10^{-12}$ m^2/s, while the permselectivity and the membrane thickness are reported in Table 2. In the case of C_{conc} = 30 g/l and C_{dil} = 0.5 g/l, by applying the Eq (9), we obtained a CCD of 3.07 A/m^2, which is equal to that found graphically.

The λ - i plot, proposed in this work to determine LCD, can also provide the CCD value: since in the critical current point the inlet and the outlet concentrations are the same, it will correspond to the zero current efficiency in the λ - i plot. For example, for inlet concentrations of 30 and 0.5 g/l, in the corresponding λ - i plot of Figure 5b, λ is zero for a current density of $\sim$3 A/m^2 that is the same value found for the CCD.

While the CCD concept has little relevance in ED fed by two solutions of equal concentrations, in the case of two feed streams at different concentrations (e.g. in a multistage ED system), a proper design must ensure that the critical current density value is easily exceeded and is sufficiently lower than the maximum (limiting) current density, so as to leave comfortable margins for a flexible operation of the unit.

5   Conclusions

In this work, experiments were carried out with an ED stack in order to determine the limiting current density. The influence of the operating conditions on LCD was studied. LCD is

influenced by the solutions' velocities but also by both streams' concentrations: indeed, non-ideal phenomena such as diffusion and osmosis, which mainly depend on concentration in the concentrate, affects the diluate concentration and, consequently, also LCD.

In the case of different inlet concentration for dilute and concentrate solutions, we observed the existence of a minimum value of current density required to desalinate a feed stream against a back-diffusion flux. Interestingly, this critical current density does not depend on the fluid velocity, but depends on the concentration difference between the concentrate and the diluate. Our one-dimensional model was validated by comparison with the experimental results. The model is very accurate in the first (linear) region, though it overestimates the values of LCD, and rather provides the (higher) diffusion-limited current density.

A review of the existing methods to determine LCD was reported. We highlighted the critical aspects of the most commonly used methods which often give ambiguous results. To overcome these issues, we proposed a new method that can provide both the limiting current density (LCD) and the critical current density (CCD). According to this method, both values are determined by plotting the current efficiency λ against the current density, where LCD is the current density at which the maximum λ occurs, while CCD corresponds to $\lambda = 0$.

Future works should further investigate the dependence of LCD (as defined by the maximum λ method) on stack features and operating conditions, and the derivation of a reliable correlation which can be used for design purposes and implemented into large-scale stack models. Moreover, further efforts should be focused on understanding (i) the reasons for the existence of a maximum in the current efficiency and (ii) the nature of limiting and overlimiting conditions, including e.g. the effects of electroconvection phenomena near membrane/solution interfaces.

Acknowledgements

Nomenclature

Symbol	Quantity	Unit
C	Bulk concentration	mol m^{-3}
D	Electrolyte diffusivity in solution	m^2 s^{-1}
D_m	Salt diffusivity in membrane	m^2 s^{-1}
F	Faraday's constant, 9.6485×10^4	C mol^{-1}
H	Thickness	m
I	Electrical current	A
i	Electrical current density	A m^{-2}
i_{lim}	Diffusion-limited current density	A m^{-2}
l	Pitch of spacers	m
L	Channel length	m
N	Molar flux	mol m^{-2} s^{-1}
Q	Volume flow rate	m^3 s^{-1}
r	Areal electrical resistance	Ω m^2
Re	Void channel Reynolds number	-
s_m	Membrane thickness	m
Sc	Schmidt number, v/D	-
Sh	Sherwood number	-
t	Transport number in solution	-
T	Transport number in membrane	-
u	Average flow velocity	m s^{-1}
V	Voltage	V

x	Co-ordinate orthogonal to membrane	m
y	Co-ordinate along the flow direction	m

Greek symbols

α	Membrane permselectivity	-
ε	Porosity, or void ratio	-
δ	Diffusion boundary layer thickness	m
Δ	Stack voltage	V
θ	Polarization coefficient	-
λ	Current Efficiency	-
v	Kinematic viscosity	$m^2\,s^{-1}$
σ	Electrical conductivity	$S\,m^{-1}$

Subscripts/superscripts

AEM	Anionic exchange membrane
CEM	Cationic exchange membrane
conc	Concentrated solution
dil	Dilute solution
DIFF	Diffusive flux
IEM	Generic membrane (AEM/CEM)
IN	Inlet
MIG	Migrative flux
OUT	Outlet
ref	Reference concentration

S	Salt	
SOL	Generic solution (concentrate/dilute)	

Acronyms

CCD	Critical current density	A m^{-2}
CFD	Computational fluid dynamics	
ED	Electrodialysis	
IEC	Ion-exchange capacity	meq g^{-1}
LCD	Limiting current density	A m^{-2}
OCV	Open circuit voltage	V
RED	Reverse electrodialysis	

References

[1]   W.G.B. Mandersloot, R.E. Hicks, Concertration polarization on ion exchange resin membranes in electrodialytic demineralization, Ind. Eng. Chem. Process Des. Dev. 4 (1965) 304–308. doi:10.1021/i260015a014.

[2]   G. Solt, Early days in electrodialysis, Desalination. 100 (1995) 15–19.

[3]   A.A. Sonin, R.F. Probstein, A hydrodynamic theory of desalination by electrodialysis, Desalination. 5 (1968) 293–329. doi:10.1016/S0011-9164(00)80105-8.

[4]   J.R. Wilson, Demineralization by electrodialysis, Butterworths Scientific Publications, 1960.

[5]   H. Jaroszek, P. Dydo, Ion-exchange membranes in chemical synthesis-a review, Open Chem. 14 (2016) 1–19. doi:10.1515/chem-2016-0002.

[6]   F. Li, W. Meindersma, A.B. De Haan, T. Reith, Optimization of commercial net spacers in spiral wound membrane modules, J. Memb. Sci. 208 (2002) 289–302. doi:10.1016/S0376-7388(02)00307-1.

[7]   H. Strathmann, Electrodialysis, a mature technology with a multitude of new applications, Desalination. 264 (2010) 268–288. doi:10.1016/j.desal.2010.04.069.

[8]   A. Campione, L. Gurreri, M. Ciofalo, G. Micale, A. Tamburini, A. Cipollina, Electrodialysis : a critical assessment an overview of recent developments on process fundamentals , models and applications, Desalination. 434 (2018) 121–160. doi:10.1016/j.desal.2017.12.044.

[9]   A.H. Galama, M. Saakes, H. Bruning, H.H.M. Rijnaarts, J.W. Post, Seawater predesalination with electrodialysis, Desalination. 342 (2014) 61–69. doi:10.1016/j.desal.2013.07.012.

[10]   H. Strathmann, Ion-Exchange Membrane Separation Processes, First ed., Elsevier, Amsterdam, 2004. doi:10.1007/s13398-014-0173-7.2.

[11]   R.K. Nagarale, G.S. Gohil, V.K. Shahi, Recent developments on ion-exchange membranes and electro-membrane processes, Adv. Colloid Interface Sci. 119 (2006) 97–130. doi:10.1016/j.cis.2005.09.005.

[12]   M. Tedesco, H.V.M. Hamelers, P.M. Biesheuvel, Nernst-Planck transport theory for (reverse) electrodialysis: I. Effect of co-ion transport through the membranes, J. Memb. Sci. 510 (2016)

370–381. doi:10.1016/j.memsci.2016.03.012.

[13]   M. Tedesco, H.V.M. Hamelers, P.M. Biesheuvel, Nernst-Planck transport theory for (reverse) electrodialysis: II. Effect of water transport through ion-exchange membranes, J. Memb. Sci. 531 (2017) 172–182. doi:10.1016/j.memsci.2017.02.031.

[14]   T. Koros, William J; MA, Y, H; Shimidzu, Terminology for Membranes and, Pure Appl. Chem. 68 (1996) 1479–1489. doi:10.1351/pac199668071479.

[15]   V. V. Nikonenko, N.D. Pismenskaya, E.I. Belova, P. Sistat, P. Huguet, G. Pourcelly, C. Larchet, Intensive current transfer in membrane systems: Modelling, mechanisms and application in electrodialysis, Adv. Colloid Interface Sci. 160 (2010) 101–123. doi:10.1016/j.cis.2010.08.001.

[16]   A.A. Sonin, M.S. Isaacson, Optimization of flow design in forced flow electrochemical systems, with special application to electrodialysis, Ind. Eng. Chem. Process Des. Dev. 13 (1974) 241–248. doi:10.1021/i260051a009.

[17]   I. Rubinstein, Electroconvection at an electrically inhomogeneous permselective interface, Phys. Fluids A Fluid Dyn. 3 (1991) 2301–2309. doi:10.1063/1.857869.

[18]   B.Y.B. Levich, The theory of concentration polarisation., Discuss. Faraday Soc. 1 (1947) 37–49.

[19]   M. Taky, G. Pourcelly, F. Lebon, C. Gavach, Polarization phenomena at the interfaces between an electrolyte solution and an ion exchange membrane. Part I. Ion transfer with a cation exchange membrane, J. Electroanal. Chem. 336 (1992) 171–194. doi:10.1016/0022-0728(92)80270-E.

[20]   M. Taky, G. Pourcelly, F. Lebon, C. Gavach, Polarization phenomena at the interfaces between an electrolyte solution and an ion exchange membrane Part II . Ion transfer with an anion exchange membrane, 336 (1992) 171–194.

[21]   A. M. Peers, General Discussion, Discuss. Faraday Soc. 21 (1956) 124.

[22]   V. V. Nikonenko, A. V. Kovalenko, M.K. Urtenov, N.D. Pismenskaya, J. Han, P. Sistat, G. Pourcelly, Desalination at overlimiting currents: State-of-the-art and perspectives, Desalination. 342 (2014) 85–106. doi:10.1016/j.desal.2014.01.008.

[23]   J. Newman, K.E. Thomas-Alyea, Electrochemical Systems, Third edit, John Wiley & Sons,

Inc., Hoboken, 2004.

[24] N.D. Pis'menskaya, V. V. Nikonenko, N. a. Mel'nik, G. Pourcelli, G. Larchet, Effect of the ion-exchange-membrane/solution interfacial characteristics on the mass transfer at severe current regimes, Russ. J. Electrochem. 48 (2012) 610–628. doi:10.1134/S1023193512060092.

[25] E.I. Belova, G.Y. Lopatkova, N.D. Pismenskaya, V. V. Nikonenko, C. Larchet, G. Pourcelly, Effect of anion-exchange membrane surface properties on mechanisms of overlimiting mass transfer, J. Phys. Chem. B. 110 (2006) 13458–13469. doi:10.1021/jp062433f.

[26] V. Geraldes, M.D. Afonso, Limiting current density in the electrodialysis of multi-ionic solutions, J. Memb. Sci. 360 (2010) 499–508. doi:10.1016/j.memsci.2010.05.054.

[27] A. Nakayama, Y. Sano, X. Bai, K. Tado, A boundary layer analysis for determination of the limiting current density in an electrodialysis desalination, Desalination. 404 (2017) 41–49. doi:10.1016/j.desal.2016.10.013.

[28] H. Schlichting, K. Gersten, Boundary-Layer Theory, (2017). doi:10.1007/978-3-662-52919-5.

[29] F. Maletzki, H.W. Rösler, E. Staude, Ion transfer across electrodialysis membranes in the overlimiting current range: stationary voltage current characteristics and current noise power spectra under different conditions of free convection, J. Memb. Sci. 71 (1992) 105–116. doi:10.1016/0376-7388(92)85010-G.

[30] I. Rubinstein, L. Shtilman, Voltage against current curves of cation exchange membranes, J. Chem. Soc. Faraday Trans. 2. 75 (1979) 231. doi:10.1039/f29797500231.

[31] I. Rubinstein, E. Staude, O. Kedem, Role of the membrane surface in concentration polarization at ion-exchange membrane, Desalination. 69 (1988) 101–114. doi:10.1016/0011-9164(88)80013-4.

[32] V. V. Nikonenko, S.A. Mareev, N.D. Pis'menskaya, A.M. Uzdenova, A. V. Kovalenko, M.K. Urtenov, G. Pourcelly, Effect of electroconvection and its use in intensifying the mass transfer in electrodialysis (Review), Russ. J. Electrochem. 53 (2017) 1122–1144. doi:10.1134/S1023193517090099.

[33] J.J. Krol, M. Wessling, H. Strathmann, Chronopotentiometry and overlimiting ion transport through monopolar ion exchange membranes, J. Memb. Sci. 162 (1999) 155–164.

doi:10.1016/S0376-7388(99)00134-9.

[34] J.J. Krol, M. Wessling, H. Strathmann, Concentration polarization with monopolar ion exchange membranes: Current-voltage curves and water dissociation, J. Memb. Sci. 162 (1999) 145–154. doi:10.1016/S0376-7388(99)00133-7.

[35] M.K. Urtenov, A.M. Uzdenova, A. V. Kovalenko, V. V. Nikonenko, N.D. Pismenskaya, V.I. Vasil'eva, P. Sistat, G. Pourcelly, Basic mathematical model of overlimiting transfer enhanced by electroconvection in flow-through electrodialysis membrane cells, J. Memb. Sci. 447 (2013) 190–202. doi:10.1016/j.memsci.2013.07.033.

[36] V.A. Shaposhnik, V.I. Vasil'eva, E. V Reshetnikova, Concentration Polarization of Ion-Exchange Membranes in Electrodialysis: An Interferometric Study, Russ. J. Electrochem. 36 (2000) 773–777.

[37] M.S. Isaacson, A.A. Sonin, Sherwood Number and Friction Factor Correlations for Electrodialysis Systems, with Application to Process Optimization, Ind. Eng. Chem. Process Des. Dev. 15 (1976) 313–321. doi:10.1021/i260058a017.

[38] V. V. Nikonenko, A.G. Istoshin, M.K. Urtenov, V.I. Zabolotsky, C. Larchet, J. Benzaria, Analysis of electrodialysis water desalination costs by convective-diffusion model, Desalination. 126 (1999) 207–211. doi:10.1016/S0011-9164(99)00176-9.

[39] H.J. Lee, F. Sarfert, H. Strathmann, S.H. Moon, Designing of an electrodialysis desalination plant, Desalination. 142 (2002) 267–286. doi:10.1016/S0011-9164(02)00208-4.

[40] H.J. Lee, H. Strathmann, S.H. Moon, Determination of the limiting current density in electrodialysis desalination as an empirical function of linear velocity, Desalination. 190 (2006) 43–50. doi:10.1016/j.desal.2005.08.004.

[41] Y. Tanaka, Concentration polarization in ion-exchange membrane electrodialysis—the events arising in a flowing solution in a desalting cell, J. Memb. Sci. 216 (2003) 149–164. doi:10.1016/S0376-7388(03)00067-X.

[42] Y. Tanaka, Limiting current density of an ion-exchange membrane and of an electrodialyzer, J. Memb. Sci. 266 (2005) 6–17. doi:10.1016/j.memsci.2005.05.005.

[43] R. Zerdoumi, K. Oulmi, S. Benslimane, Electrochemical characterization of the CMX cation

exchange membrane in buffered solutions: Effect on concentration polarization and counterions transport properties, Desalination. 340 (2014) 42–48. doi:10.1016/j.desal.2014.02.014.

[44] P. Długołęcki, B. Anet, S.J. Metz, K. Nijmeijer, M. Wessling, P. Długołecki, B. Anet, S.J. Metz, K. Nijmeijer, M. Wessling, Transport limitations in ion exchange membranes at low salt concentrations, J. Memb. Sci. 346 (2010) 163–171. doi:10.1016/j.memsci.2009.09.033.

[45] J.-H.H. Choi, S.-H.H. Kim, S.-H.H. Moon, Heterogeneity of ion-exchange membranes: The effects of membrane heterogeneity on transport properties, J. Colloid Interface Sci. 241 (2001) 120–126. doi:10.1006/jcis.2001.7710.

[46] J. Balster, I. Pünt, D.F. Stamatialis, M. Wessling, Multi-layer spacer geometries with improved mass transport, J. Memb. Sci. 282 (2006) 351–361. doi:10.1016/j.memsci.2006.05.039.

[47] D.A. Cowan, J.H. Brown, Effect of Turbulence on Limiting Current in Electrodialysis Cells, Ind. Eng. Chem. 51 (1959) 1445–1448. doi:10.1021/ie50600a026.

[48] E. V. Laktionov, N.D. Pismenskaya, V. V. Nikonenko, V.I. Zabolotsky, Method of electrodialysis stack testing with the feed solution concentration regulation, Desalination. 151 (2003) 101–116. doi:10.1016/S0011-9164(02)00988-8.

[49] D.A. Vermaas, M. Saakes, K. Nijmeijer, Enhanced mixing in the diffusive boundary layer for energy generation in reverse electrodialysis, J. Memb. Sci. 453 (2014) 312–319. doi:10.1016/j.memsci.2013.11.005.

[50] M. La Cerva, M. Di Liberto, L. Gurreri, A. Tamburini, A. Cipollina, G. Micale, M. Ciofalo, Coupling CFD with a one-dimensional model to predict the performance of reverse electrodialysis stacks, J. Memb. Sci. 541 (2017) 595–610. doi:10.1016/j.memsci.2017.07.030.

[51] K.S. Pitzer, Thermodynamics of electrolytes. I. Theoretical basis and general equations, J. Phys. Chem. 77 (1973) 268–277. doi:10.1021/j100621a026.

[52] K.S. Pitzer, G. Mayorga, Thermodynamics of electrolytes. II. Activity and osmotic coefficients for 2-2 electrolytes, J. Solution Chem. 3 (1974) 539–546. doi:10.1007/BF00648138.

[53] L. Gurreri, G. Battaglia, A. Tamburini, A. Cipollina, G. Micale, M. Ciofalo, Multi-physical modelling of reverse electrodialysis, Desalination. 423 (2017) 52–64. doi:10.1016/j.desal.2017.09.006.

[54] A. Tamburini, G. La Barbera, A. Cipollina, M. Ciofalo, G. Micale, CFD simulation of channels for direct and reverse electrodialysis, Desalin. Water Treat. 48 (2012) 370–389. doi:10.1080/19443994.2012.705084.

[55] L. Gurreri, A. Tamburini, A. Cipollina, G. Micale, M. Ciofalo, Flow and mass transfer in spacer-filled channels for reverse electrodialysis: a CFD parametrical study, J. Memb. Sci. 497 (2016) 300–317. doi:10.1016/j.memsci.2015.09.006.

[56] V. V. Nikonenko, N.D. Pismenskaya, A.G. Istoshin, V.I. Zabolotsky, A.A. Shudrenko, Description of mass transfer characteristics of ED and EDI apparatuses by using the similarity theory and compartmentation method, Chem. Eng. Process. Process Intensif. 47 (2008) 1118–1127. doi:10.1016/j.cep.2007.12.005.

[57] D.W. Green, R.H. Perry, Perry's Chemical Engineers' Handbook, eighth, McGraw-Hill, New York, 2007.

[58] V. Vitagliano, P. a Lyons, Diffusion coefficients for aqueous solutions of sodium chloride and barium chloride, J. Am. Chem. Soc. 76 (1956) 1549–1552. doi:10.1021/ja01589a011.

[59] M. Tedesco, A. Cipollina, A. Tamburini, I.D.L. Bogle, G. Micale, A simulation tool for analysis and design of reverse electrodialysis using concentrated brines, Chem. Eng. Res. Des. 93 (2015) 441–456. doi:10.1016/j.cherd.2014.05.009.

[60] S.S. Islam, R.L. Gupta, K. Ismail, Extension of the Falkenhagen-Leist–Kelbg Equation to the Electrical Conductance of Concentrated Aqueous Electrolytes, J. Chem. Eng. Data. 36 (1991) 102–104. doi:10.1021/je00001a031.

[61] H. Meng, D. Deng, S. Chen, G. Zhang, A new method to determine the optimal operating current (Ilim′) in the electrodialysis process, Desalination. 181 (2005) 101–108. doi:10.1016/j.desal.2005.01.014.

[62] L.H. Shaffer, M.S. Mintz, Electrodialysis, in: Princ. Desalin., 2nd Ed., Academic Press Inc., New York, 1980. doi:10.1016/B978-0-12-801764-7/00006-1.

[63] R. Kwak, G. Guan, W.K. Peng, J. Han, Microscale electrodialysis: Concentration profiling and vortex visualization, Desalination. 308 (2013) 138–146. doi:10.1016/j.desal.2012.07.017.

[64] F. Li, W. Meindersma, A.B. De Haan, T. Reith, Experimental validation of CFD mass transfer

simulations in flat channels with non-woven net spacers, J. Memb. Sci. 232 (2004) 19–30. doi:10.1016/j.memsci.2003.11.015.

[65] C.P. Koutsou, S.G. Yiantsios, A.J. Karabelas, Direct numerical simulation of flow in spacer-filled channels: Effect of spacer geometrical characteristics, J. Memb. Sci. 291 (2007) 53–69. doi:10.1016/j.memsci.2006.12.032.